



Cite this: *Chem. Commun.*, 2015, 51, 1811

Received 30th October 2014,  
Accepted 10th December 2014

DOI: 10.1039/c4cc08602c

www.rsc.org/chemcomm

# Self-organization of star-shaped columnar liquid crystals with a coaxial nanophase segregation revealed by a combined experimental and simulation approach†

Eduardo Beltrán,<sup>a</sup> Matteo Garzoni,<sup>b</sup> Beatriz Feringán,<sup>a</sup> Alberto Vancheri,<sup>b</sup> Joaquín Barberá,<sup>a</sup> José Luis Serrano,<sup>c</sup> Giovanni M. Pavan,<sup>\*b</sup> Raquel Giménez<sup>\*a</sup> and Teresa Sierra<sup>\*a</sup>

**Fully consistent X-ray data and molecular dynamics simulations on new star-shaped liquid crystals yield two nanosegregated architectures with a coaxial stacking of two functional discotic units: tris(triazolyl)triazine and triphenylene. Analysis of lattice order along the principal axes reveals preferential staggered arrangement of the stacked molecules in the columnar assembly.**

Molecularly engineered systems able to organize spontaneously in domains with different functionalities at the nanoscale are promising candidates for miniaturized optoelectronic devices.<sup>1</sup> One strategy to control phase separation at the nanometer scale is to rely on the self-organization of columnar liquid crystals. These are systems able to stack spontaneously into columns, leading to one-dimensional materials.<sup>2</sup> A conveniently designed columnar liquid crystal with different functional units covalently grafted to their molecular structure can lead to a coaxial assembly allowing, in principle, to control the phase segregation with nanoscale precision.<sup>1d,3</sup> However, this is not an easy task as high control over face stacking to avoid mixed columns is needed for this purpose.

We have previously described a novel electron-deficient and luminescent star-shaped tris(triazolyl)triazine platform,<sup>4</sup> which has a strong tendency to self-organize in hexagonal columnar mesophases with different arrangements as consequence of the flexibility of the polar triazole-containing branches.<sup>4b</sup> The one-pot synthetic procedure used to build this tris(triazolyl)triazine core, which is based on click chemistry methods,<sup>5</sup> makes straightforward its

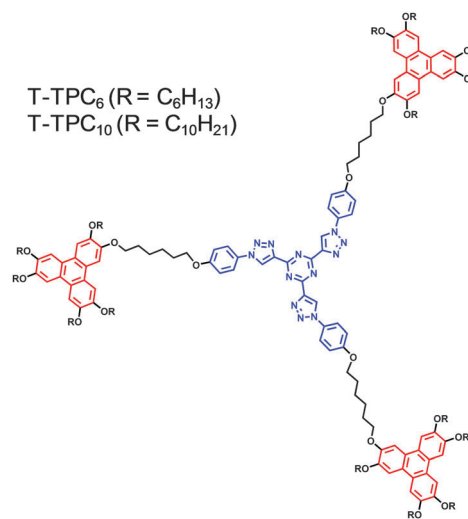


Fig. 1 Schematic drawing of the compounds studied in this work.

functionalization with peripheral discotic electron-rich triphenylenes (Fig. 1). In this way, two compounds have been prepared, *i.e.*, **T-TPC<sub>6</sub>**, with terminal hexyloxy chains, and **T-TPC<sub>10</sub>**, with decyloxy chains. In both cases the triphenylene units (red) are grafted to the tris(triazolyl)triazine core (blue) by means of an hexamethylene spacer (see synthetic details in the ESI†). These supermolecules self-organize in two different ways, both based on coaxial columns made of a single type of discotic unit. The self-assembled structure of these materials has been characterized by the synergic use of X-ray experiments (XRD) and molecular dynamics (MD) simulations.

The study of the mesomorphic behavior concludes that both compounds show a columnar liquid crystal phase (Table S1, ESI†). The mesophase of **T-TPC<sub>6</sub>** develops on cooling at 90 °C with a homeotropic texture (black between cross-polarizers). The tendency to spontaneous homeotropic alignment (columns normal to surfaces) is an important property for some device implementation. In contrast, compound **T-TPC<sub>10</sub>** shows a birefringent texture on cooling from 118 °C (Fig. S1, ESI†).

<sup>a</sup> Departamento de Química Orgánica, Instituto de Ciencia de Materiales de Aragón (ICMA) - Universidad de Zaragoza-CSIC, 50009 Zaragoza, Spain.  
E-mail: rgimenez@unizar.es, tsierra@unizar.es

<sup>b</sup> Department of Innovative Technologies, University of Applied Sciences and Arts of Southern Switzerland, Galleria 2, Manno 6928, Switzerland.  
E-mail: giovanni.pavan@supsi.ch; Tel: +41 58 666 6676

<sup>c</sup> Departamento de Química Orgánica, Instituto de Nanociencia de Aragón. Universidad de Zaragoza, C/ Mariano Esquillor, 50018 Zaragoza, Spain

† Electronic supplementary information (ESI) available: Synthesis and characterization data, computational methods and additional material from the simulations. See DOI: 10.1039/c4cc08602c

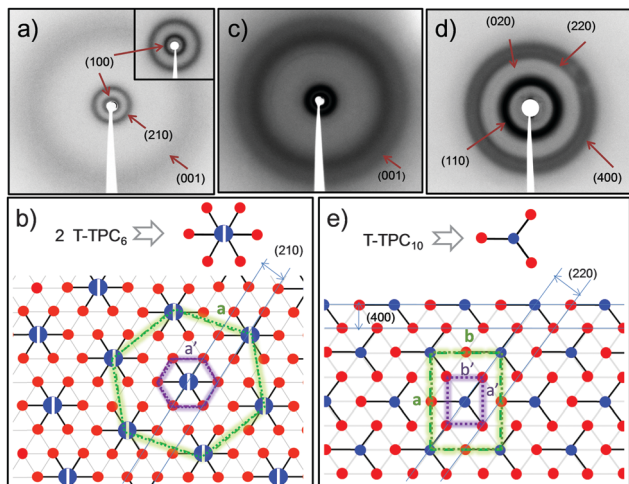


**Fig. 2** (a) XRD diffractogram of **T-TPC<sub>6</sub>**, inset shows a magnification of the low-angle region. (b) Self-assembly model for **T-TPC<sub>6</sub>**. (c) XRD diffractogram of **T-TPC<sub>10</sub>** and (d) low-angle region of the XRD diffractogram of **T-TPC<sub>10</sub>**; (e) self-assembly model for **T-TPC<sub>10</sub>**. In (b) and (e), red and blue dots represent the centers of the columns (see ESI†).

XRD diffractograms of **T-TPC<sub>6</sub>** (Fig. 2a) display two reflections in the low-angle region which are in a relationship  $1 : 1\sqrt{7}$ . In addition, a broad, diffuse halo at  $4.6 \text{ \AA}$  is observed in the high-angle region, typical of the conformational disorder of the aliphatic chains of the liquid crystalline state, with an intensity reinforcement in the outer border at  $c = 4.1 \text{ \AA}$ , which corresponds to the intracolumnar stacking order. The two low-angle reflections can be assigned to the reflections (100) and (210) of a two-dimensional hexagonal network with a parameter  $a = 52.6 \text{ \AA}$ . The intensity of both reflections is almost the same, but the latter is unusually intense. This means that there is a strong modulation of the electronic density with a period of  $\sqrt{7}$  times shorter than the (100) spacing and suggests the existence of an additional network or sublattice formed by locally packed triphenylene columns with a hexagonal symmetry (Fig. 2b).<sup>6</sup> Taking into account the cell volume of the hexagonal network, and assuming that the density of the material is close to  $0.9\text{--}1 \text{ g cm}^{-3}$ , the cell unit should contain two molecules of **T-TPC<sub>6</sub>** to achieve an efficient space filling. Following this data, we can propose a model for the organization of **T-TPC<sub>6</sub>** in the mesophase (Fig. 2b) in which two antiparallel supermolecules in a non-star conformation can accommodate in a columnar stratum and stack constituting the main hexagonal network (green hexagon). In this situation, six triphenylene moieties must be arranged at the periphery of the main column in such a way that they form a hexagonal sublattice (purple hexagon) which is in relationship  $a' = a/\sqrt{7}$ . The sublattice parameter  $a'$  fits the hexagonal cell parameter found for the columnar mesophase generated by hexahydroxytriphenylene ( $20.0 \text{ \AA}$ ). Nevertheless, the sublattice is not homogeneous as it is constituted by six triphenylene columns (represented by red dots) around one column of tris(triazolyl)triazine dimers (represented by two blue half-disks), or by five triphenylene columns and one column of tris(triazolyl)triazine dimer around a triphenylene column.

Compound **T-TPC<sub>10</sub>**, with the same spacer but with decyloxy terminal chains in the triphenylene unit, shows a different

diffractogram containing a set of reflections in the low angle region that can be indexed to a rectangular network with parameters  $a = 80.2 \text{ \AA}$  and  $b = 58.0 \text{ \AA}$  (Fig. 2c and d). The rectangular symmetry can be assigned to a distorted hexagonal lattice. The distortion could be associated to a tilting of the discotic units; however no information about this can be drawn from the X-ray measurements. In the wide angle region the broad halo corresponding to the terminal chains in a disordered conformational state and an additional halo at  $c = 3.5 \text{ \AA}$  (intracolumnar stacking order) are clearly visible. The first, third and fourth reflections of the low angle region are strong, which indicates a reinforcement of the electronic density along the planes (110), (220) and (400). The first corresponds to the main nodes of the network, but the other ones reveal existence of a strong modulation of the electronic density with wavelengths corresponding to the intercolumnar distances between triphenylene moieties. This suggests that, in addition to the main rectangular network formed by the supermolecule (green rectangle in Fig. 2e), the peripheral triphenylenes pack to generate a sublattice. Taking into account the measured parameters of the rectangular columnar mesophase and assuming that the density of the material is close to  $0.9\text{--}1 \text{ g cm}^{-3}$ , in this case we obtain that each node of the main rectangular lattice contains a single supermolecule. Moreover, the fact that reflection (220) is strong suggests that the triphenylene columns lie on these planes, and that each **T-TPC<sub>10</sub>** supermolecule has its three triphenylenes radiating at  $\approx 120^\circ$  and interdigitating with the triphenylenes from the neighbouring supermolecules (Fig. 2e). In fact the (220) is equivalent to the (110) reflection of a sublattice with  $a' = a/2$  and  $b' = b/2$  containing locally packed columns in the centre and in the corner (purple rectangle). Similar reasoning can be made about the (400) reflection, which is equivalent to the (200) reflection of the sublattice. Both families of planes (220) and (400) are generated by close-packed columns and thus they contain a high electronic density (Fig. 2e).

All obtained X-ray patterns show that the first reflection is the strongest one, indicating that for both compounds the supermolecule is the main unit in the lattice rather than the constituent triphenylene or tris(triazolyl)triazine disks. This is in contrast with previously reported columnar mesophases of star-shaped supermolecules with peripheral triphenylenes. For example, in the case of supermolecules with porphyrin<sup>7</sup> or 1,3,5-benzenetrisamide<sup>8</sup> cores it was demonstrated that the main lattice is formed by the surrounding triphenylene units. In both the **T-TPC<sub>6</sub>** and **T-TPC<sub>10</sub>** cases, the supermolecules are stacked along the  $z$ -axis and the triphenylene units form a sublattice around the cores on the  $xy$  plane, which is consistent with a nanophase segregation in columns.

MD simulations were carried out to further investigate the proposed self-assembly models, and to study the levels of order inside the lattice on the  $xy$  plane and along the  $z$  axis (stacking). To tackle these points, two different symmetric self-assembled configurations were considered to build the starting atomistic models of each compound, differing in the relative orientation of the molecules in the columns (rotation around the  $z$  axis). The two starting configurations for the **T-TPC<sub>10</sub>** system, both consistent with the rectangular lattice symmetry reported by the XRD data (Fig. 2e), are **T-TPC<sub>10</sub>-0°** (Fig. 3a), having all molecules perfectly superimposed inside the columns ( $0^\circ$  rotation along the  $z$  axis), and **T-TPC<sub>10</sub>-180°**,

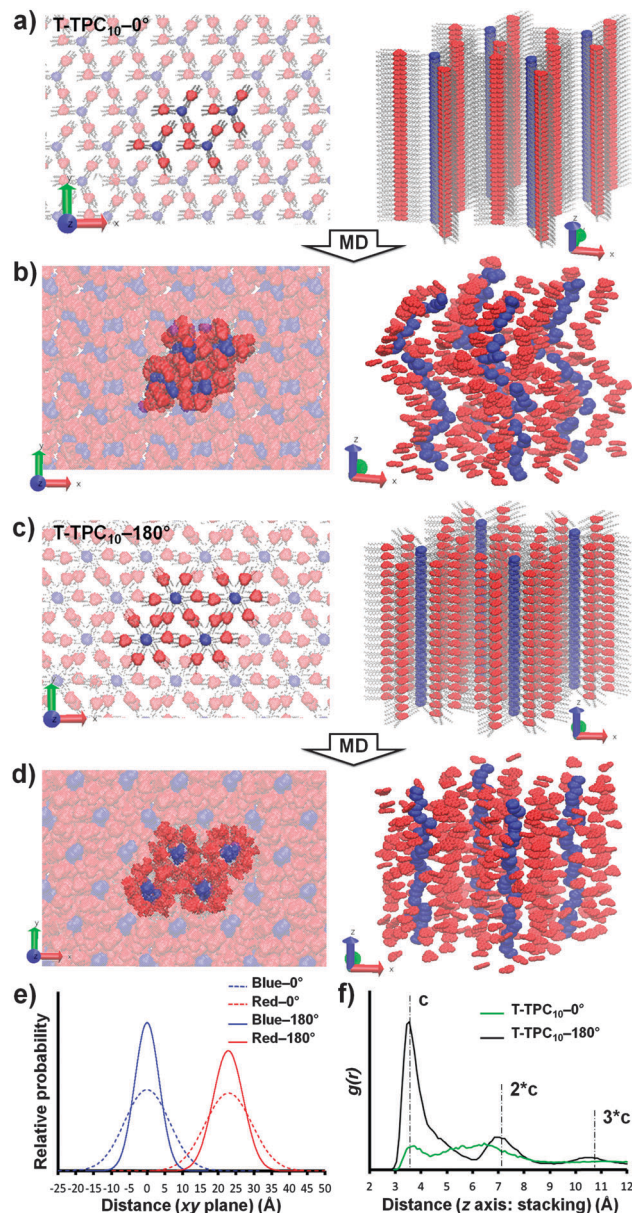


Fig. 3 MD simulations of the **T-TPC<sub>10</sub>** systems. Top and side views: starting (a) and equilibrated configurations (b) of the **T-TPC<sub>10</sub>-0°** system. (c) Starting and equilibrated (d) configurations of the **T-TPC<sub>10</sub>-180°** system. (e) Gaussian distributions of blue and red groups (CM) on the *xy* plane. (f) Radial distribution functions (*g(r)*) of the cores used to assess stacking order along the *z* axis.

with molecules rotated by 180°, leading to a staggered arrangement along the *z* axis (Fig. 3c). For **T-TPC<sub>6</sub>**, the two selected configurations are **T-TPC<sub>6</sub>-0°**, having all molecules perfectly superimposed along the *z* axis (0° rotation), and **T-TPC<sub>6</sub>-60°**, where molecules are rotated by 60° in the columns. Importantly, in the **T-TPC<sub>6</sub>** system only the stacking of the dimeric cores is different between the 0° and 60° configurations (Fig. 4a and b: left), while both dispositions are consistent with the hexagonal symmetry of the lattice reported by the XRD experiments (Fig. 2b).

Since each simulated system starts from an ideal configuration consistent with the experiments and evolves toward the equilibrium during the MD run, the comparison between the rotated and the

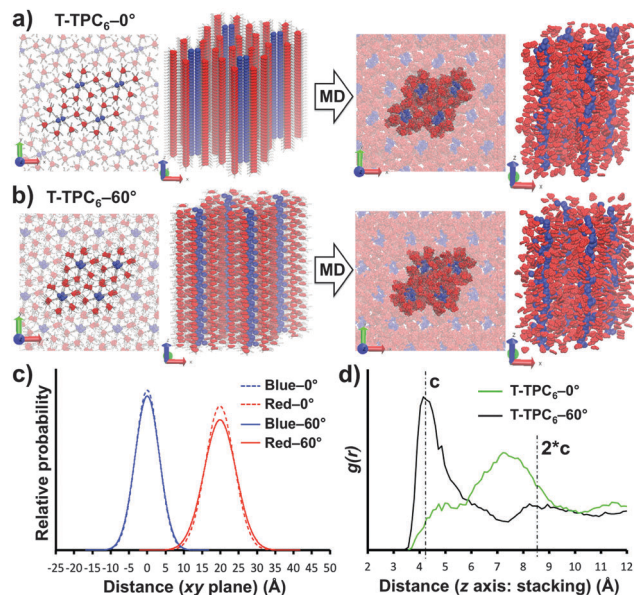


Fig. 4 MD simulations of the **T-TPC<sub>6</sub>** systems. Top and side views: ideal starting (left) and equilibrated configurations (right) of the **T-TPC<sub>6</sub>-0°** (a) and **T-TPC<sub>6</sub>-60°** (b) systems. (c) Gaussian distributions of blue and red groups (CM) on the *xy* plane. (d) Radial distribution functions (*g(r)*) of the molecular cores used to assess stacking order along the *z* axis.

superimposed systems allows understanding which assembly scheme is more stable during the simulations. Namely, if during the MD one system evolves to an equilibrated configuration that strongly deviates from the starting one, this means that the ideal configuration initially proposed was unrealistic for that system.

The simulation approach adopted herein is similar to that used to study similar complex self-assembled nanostructures.<sup>9</sup> All simulated molecular systems consist of four pre-assembled columns each containing 72 **T-TPC<sub>6</sub>** (two in each node) and 36 **T-TPC<sub>10</sub>** pre-stacked and initially extended supermolecules arranged in space according to the lattice parameters (*a* and *c* for the hexagonal lattice, or *a*, *b* and *c* for the rectangular one) from the XRD experiments (Fig. 3a, c and 4a, b). All MD simulations were conducted in periodic boundary conditions, so that the molecular systems replicated in space are representative of the bulk ordered phase of the liquid crystals. Analysis of the lattice parameters (*a*, *b* and *c*) of the molecular systems obtained from MD at the equilibrium demonstrates very good consistency between the models and the experiments (extensive computational details are provided in the ESI†).

For the best clarity, the results obtained from the MD simulations will be presented first for **T-TPC<sub>10</sub>** and then for the **T-TPC<sub>6</sub>** system.

The MD simulations of **T-TPC<sub>10</sub>** show that at the equilibrium the **T-TPC<sub>10</sub>-0°** system deviates from the initial (ideal) configuration much more than the **T-TPC<sub>10</sub>-180°** staggered one. The **T-TPC<sub>10</sub>-0°** distortion is evident by looking at the columnar stacking of the blue cores (Fig. 3b). Conversely, the ideal lattice columnar assembly is much more preserved at the equilibrium in the **T-TPC<sub>10</sub>-180°** case (Fig. 3d). This indicates that the initial superimposed (0°) assembled configuration is less stable than the staggered one (180°) for the **T-TPC<sub>10</sub>** system, which is consistent with the less uniform atom density initially present in the **T-TPC<sub>10</sub>-0°** lattice compared to **T-TPC<sub>10</sub>-180°**.

From the equilibrated phase MD trajectories, we extracted information on the relative space displacement (distributions on the  $xy$  plane and along the  $z$  axis) of the blue and red groups centers of mass (CM) of the **T-TPC**<sub>10</sub> molecules in the two systems. Shown in Fig. 3e, the Gaussian distributions of blue and red groups on the  $xy$  plane are clearly broader for **T-TPC**<sub>10</sub>-0° than in the case of **T-TPC**<sub>10</sub>-180°. The positions of the Gaussian peaks indicate the most probable distances between blue and red group centers on the  $xy$  plane in equilibrium conditions, which are well consistent with the lattice results from the XRD experiments (see ESI†). The height of the Gaussians is indicative of the relative probability of finding blue or red groups in the experimental positions on the  $xy$  plane rather than far from them. Thus, these data quantify how well the two models reproduce the experimental (XRD) lattice of Fig. 2e on the  $xy$  plane. The red and blue Gaussian peaks are almost twice higher when the **T-TPC**<sub>10</sub> molecules are rotated by 180° (solid lines) rather than perfectly superimposed (0°: dotted lines) in the columns, demonstrating that the **T-TPC**<sub>10</sub>-180° assembly is much more consistent with the XRD experiments than **T-TPC**<sub>10</sub>-0°.

In addition, information on the stacking order along the  $z$  axis can be inferred from the radial distribution functions ( $g(r)$ ) of the cores. Analysis of the  $g(r)$  of **T-TPC**<sub>10</sub>-180° (Fig. 3f, black curve) shows a clear high first peak at distance consistent with the experimental stacking one ( $c = 3.5$  Å), and successive peaks with reduced height at intercore distances multiple of  $c$ . Since  $g(r)$  data are indicative of the relative probability of finding cores in space as a function of the intercore distance, these results reveal the presence of short-range regular stacking in the **T-TPC**<sub>10</sub>-180° staggered system consistent with the XRD experiments. On the contrary, the same evidence of regular stacking is not present in the case of the superimposed **T-TPC**<sub>10</sub>-0° system (Fig. 3f, green curve). Altogether, these results demonstrate that, at the molecular level, the ordered lattice reported by the XRD experiments for **T-TPC**<sub>10</sub> is consistent with an assembled structure where the molecules self-organize along the  $z$  axis into a staggered configuration (180° intermolecular rotation) rather than in columns with  $C_3$  molecules perfectly superimposed (0°).

MD simulations of the **T-TPC**<sub>6</sub> systems also produced interesting insight (Fig. 4). Both equilibrated configurations of **T-TPC**<sub>6</sub>-60° and **T-TPC**<sub>6</sub>-0° show similar displacement of the red and blue groups on the  $xy$  plane, as demonstrated by nearly identical Gaussians for the rotated (60°) and superimposed (0°) systems (Fig. 4c). This is reasonable since in this case, differently from the **T-TPC**<sub>10</sub> system, a rigid 60° rotation of the molecules around the  $z$  axis does not produce considerable differences in terms of atom density inside the lattice between **T-TPC**<sub>6</sub>-60° and **T-TPC**<sub>6</sub>-0°.

However, interestingly, analysis of the  $g(r)$  curves of the **T-TPC**<sub>6</sub> cores shows remarkable difference between the two self-assembled structures along the  $z$  axis (Fig. 4d). In fact, the first high peak found in the  $g(r)$  of the rotated **T-TPC**<sub>6</sub>-60° system (Fig. 4d, black) indicates presence of regular stacking consistent with the XRD experiments ( $c = 4.1$  Å). In contrast, this is absent for **T-TPC**<sub>6</sub>-0° (Fig. 4d, green curve). As a summary, even if in the real fluid system both rotated and superimposed configurations can coexist to some extent, these results demonstrate that, also in this case, the ordered lattice reported by XRD experiments is more probably formed by columns where **T-TPC**<sub>6</sub> dimers are self-organized with 60° rotation one

respect to each other rather than perfectly superimposed along the  $z$  axis.

In conclusion, a new class of self-organized systems leading to coaxial nanosegregation have been described. These are based on two chemically different discotic units with a tris(triazolyl)triazine star-shaped core linked by a flexible spacer to three pentaalkoxy-triphenylenes. The length of the terminal alkoxy chains plays an important role in the supramolecular organization leading to different self-organization modes.

MD simulations of the self-assembled systems starting from two possible ideal lattices consistent with the experiments, where **T-TPC**<sub>6</sub> and **T-TPC**<sub>10</sub> units are perfectly superimposed (0°) or symmetrically rotated along the  $z$  axis (60° or 180°, respectively), show that in both cases the supermolecules are likely self-assembled by rotated stacking along the  $z$  axis.

The synergy between XRD experiments and MD simulations reported herein allows for a unique and comprehensive characterization of these self-assembled structures, proposing a new combined theoretical-experimental approach for the rational design of new self-assembling functional nanomaterials.

This work was financially supported by the MINECO-FEDER funds (projects MAT2012-38538-CO3-01, CTQ2012-35692, FPI fellowship to E.B.), and the Gobierno de Aragón-FSE (E04 research group, fellowship to B.F.). Authors would like to acknowledge the Servicio General de Apoyo a la Investigación-SAI and CEQMA, Universidad de Zaragoza -CSIC.

## Notes and references

- (a) V. Percec, M. Glodde, T. K. Beta, Y. Miura, I. Shiyonovskaya, K. D. Singer, V. S. K. Balagurusamy, P. A. Heiney, I. Schnell, A. Rapp, H. W. Spiess, S. D. Hudson and H. Duan, *Nature*, 2002, **419**, 384; (b) Y. Yamamoto, G. Zhang, W. Jin, T. Fukushima, N. Ishii, A. Saeki, S. Seki, S. Tagawa, T. Minari, K. Tsukagoshi and T. Aida, *Proc. Natl. Acad. Sci. U. S. A.*, 2009, **106**, 21051; (c) T. Aida, E. W. Meijer and S. I. Stupp, *Science*, 2012, **335**, 813; (d) J. M. Mativetsky, M. Kastler, R. C. Savage, D. Gentilini, M. Palma, W. Pisula, K. Müllen and P. Samori, *Adv. Funct. Mater.*, 2009, **19**, 2486.
- Y. Shimizu, in *Supramolecular Soft Matter: Applications in Materials and Organic Electronics*, ed. T. Nakanishi, John Wiley and Sons, 2011, pp. 345–360.
- (a) H. Hayashi, W. Nihashi, T. Umeyama, Y. Matano, S. Seki, Y. Shimizu and H. Imahori, *J. Am. Chem. Soc.*, 2011, **133**, 10736; (b) P. Samori, X. Yin, N. Tehebotareva, Z. Wang, T. Pakula, F. Jäckel, M. D. Watson, A. Venturini, K. Müllen and J. P. Rabe, *J. Am. Chem. Soc.*, 2004, **126**, 3567.
- (a) E. Beltrán, J. L. Serrano, T. Sierra and R. Giménez, *Org. Lett.*, 2010, **7**, 1404; (b) E. Beltrán, J. L. Serrano, T. Sierra and R. Giménez, *J. Mater. Chem.*, 2012, **22**, 7797.
- H. C. Kolb, M. G. Finn and K. B. Sharpless, *Angew. Chem., Int. Ed.*, 2001, **40**, 2004.
- (a) M. D. McKenna, J. Barberá, M. Marcos and J. L. Serrano, *J. Am. Chem. Soc.*, 2005, **127**, 619; (b) A. Zelcer, B. Donnio, C. Bourgoigne, F. D. Cukiernik and D. Guillon, *Chem. Mater.*, 2007, **19**, 1992.
- J. Miao and L. Zhu, *Soft Matter*, 2010, **6**, 2072.
- (a) I. Paraschiv, M. Giesbers, B. Van Lagen, F. C. Grozema, R. D. Abellon, L. D. A. Siebbeles, A. T. M. Marcelis, H. Zuilhof and E. J. R. Sudhölter, *Chem. Mater.*, 2006, **18**, 968; (b) I. Paraschiv, K. De Lange, M. Giesbers, B. Van Lagen, F. C. Grozema, R. D. Abellon, L. D. A. Siebbeles, E. J. R. Sudhölter, H. Zuilhof and A. T. M. Marcelis, *J. Mater. Chem.*, 2008, **18**, 5475.
- (a) X. L. Feng, V. Marcon, W. Pisula, M. R. Hansen, J. Kirkpatrick, F. Grozema, D. Andrienko, K. Kremer and K. Müllen, *Nat. Mater.*, 2009, **8**, 421; (b) G. Doni, M. D. Nkoua Ngavouka, A. Barducci, P. Parisse, A. De Vita, G. Scoles, L. Casalis and G. M. Pavan, *Nanoscale*, 2013, **5**, 9988.